Harjuoja, J., Väyrynen, S., Putkonen, M., Niinistö, L., and Rauhala, E., Crystallization of bismuth titanate and bismuth silicate grown as thin films by atomic layer deposition, Journal of Crystal Growth 286 (2006) 376-383.

© 2006 Elsevier Science

Reprinted with permission.

Available online at www.sciencedirect.com
SCIENCE DIRECT
ELSEVIER
Journal of Crystal Growth 286 (2006) 376–383
JOURNAL OF CRYSTAL GROWTH
www.elsevier.com/locate/jcrysgro

Crystallization of bismuth titanate and bismuth silicate grown as thin films by atomic layer deposition

Jenni Harjuoja[a,*], Samuli Väyrynen[b], Matti Putkonen[a], Lauri Niinistö[a], Eero Rauhala[b]

[a]Laboratory of Inorganic and Analytical Chemistry, Helsinki University of Technology, P.O. Box 6100, FIN-02015 Espoo, Finland
[b]Accelerator Laboratory, University of Helsinki, P.O. Box 43, FIN-00014, Finland

Received 1 September 2005; received in revised form 5 October 2005; accepted 12 October 2005

Communicated by M. Kawasaki

Abstract

Bismuth silicate and bismuth titanate thin films were deposited by atomic layer deposition (ALD). A novel approach with pulsing of two Bi-precursors was studied to control the Si/Bi atomic ratio in bismuth silicate thin films. The crystallization of compounds formed in the Bi_2O_3–SiO_2 and Bi_2O_3–TiO_2 systems was investigated. Control of the stoichiometry of Bi–Si–O thin films was studied when deposited on Si(1 0 0) and crystallization was studied for films on sapphire and MgO-, ZrO_2- and YSZ-buffered Si(1 0 0). The Bi–Ti–O thin films were deposited on Si(1 0 0) substrate. Both Bi–Si–O and Bi–Ti–O thin films were amorphous after deposition. Highly *a*-axis oriented Bi_2SiO_5 thin films were obtained when the Bi–Si–O thin films deposited on MgO-buffered Si(1 0 0) were annealed at 800 °C in nitrogen. The full-width half-maximum values for 200 peak were also studied. An excess of bismuth was found to improve the crystallization of Bi–Ti–O thin films and the best crystallinity was observed with Ti/Bi atomic ratio of 0.28 for films annealed at nitrogen at 1000 °C. Roughness of the thin films as well as the concentration depth distribution were also examined.
© 2005 Elsevier B.V. All rights reserved.

PACS: 81.15.Gh

Keywords: A1. Crystal structure; A3. Atomic layer deposition; B1. Bismuth compounds; B1. Oxides; B2. Ferroelectric material

1. Introduction

There exist a large number of crystalline compounds in the Bi_2O_3–SiO_2 and Bi_2O_3–TiO_2 systems [1–5]. Ternary bismuth compounds form a variety of phases such as Bi_2SiO_5, $Bi_4Si_3O_{12}$, $Bi_{12}SiO_{20}$, $Bi_2Ti_2O_7$, $Bi_4Ti_3O_{12}$ and $Bi_{12}TiO_{20}$. These phases have been deposited by both chemical and physical methods [1–20]. For example, Bi_2SiO_5 has attracted interest as buffer layer for metal–ferroelectric–insulator–semiconductor (MIS) structures [1,22]. $Bi_4Si_3O_{12}$ (eulytite) has been examined for dynamic random access memories (DRAM) and for use as buffer layers in the growth of other oxide films on Si [7]. $Bi_{12}SiO_{20}$ (sillenite) and $Bi_{12}TiO_{20}$ are both optically active materials and have been reported to be potential material choices for electro-optics [10,23,24]. $Bi_4Ti_3O_{12}$ is a typical ferroelectric material and it has therefore been studied for nonvolatile memories [19,25] and electro-optic devices [17]. Recently $Bi_4Ti_3O_{12}$ has been studied as a base material for ferroelectric memories where thin film properties were modified by incorporating a suitable rare earth cation into the $Bi_4Ti_3O_{12}$ lattice [26]. Due to its relatively high permittivity and low leakage current [3,11], $Bi_2Ti_2O_7$ has been introduced as a new material in advanced MOSFET transistors. This structure has also been used as a buffer layer for $Bi_4Ti_3O_{12}$ [1,27] and lead zirconate titanate (PZT) [28] thin films.

Chemical deposition methods usually produce amorphous films when low deposition temperatures are used and therefore annealing is required to obtain crystalline and oriented films. Typical annealing temperatures for Bi–Si–O thin films have been between 650 and 725 °C in O_2 atmosphere [1,2,10]. While Bi–Ti–O thin films have been

*Corresponding author. Tel.: +358 9 4512596; fax: +358 9 462373.
E-mail address: jenni.harjuoja@tkk.fi (J. Harjuoja).

0022-0248/$ - see front matter © 2005 Elsevier B.V. All rights reserved.
doi:10.1016/j.jcrysgro.2005.10.020

annealed at 630–850 °C [1,12,16], polycrystalline thin films have been obtained even at 550 °C [3,23]. Atmospheres used in annealing of Bi–Ti–O phases have been oxygen or air [1,3]. Another possibility is to use high enough deposition temperatures as done in MOCVD to obtain the as-deposited thin films crystalline [4,7,14,15,22,29].

Different crystalline phases could also simultaneously exist depending on the composition as well as on the annealing and deposition temperatures. Crystallization could also be incomplete and then amorphous material is present along the crystalline phase [30]. For example, crystallization of $Bi_4Ti_3O_{12}$ thin films has been studied by varying the stoichiometry of the CVD-deposited films. Excess amount of bismuth has been reported to improve the $Bi_4Ti_3O_{12}$ crystallization [4] although other phases may be present, namely $Bi_{12}TiO_{20}$ [13]. On the other hand, low bismuth content resulted in the formation of $Bi_2Ti_2O_7$ (pyrochlore) phase alone [4] or together with the $Bi_4Ti_3O_{12}$ phase [5] or $Bi_4Ti_3O_{12}$ together with TiO_2 [13]. Sun et al. [4] found that even when the right composition of bismuth and titanium was used, small amounts of the pyrochlore phase was present.

Several authors have observed that the crystalline orientations of Bi–Si–O and Bi–Ti–O thin films are influenced by the deposition or annealing temperature. Although crystalline $Bi_4Si_3O_{12}$ phase starts forming at 780 °C [31], pure polycrystalline $Bi_4Si_3O_{12}$ phase was observed only at 820 °C. In the case of bismuth titanate, Wang et al. [20] studied the influence of annealing temperature on the crystalline properties of $Bi_4Ti_3O_{12}$ thin films. After annealing at 600 °C, the films showed a mixed phase structure consisting of $Bi_4Ti_3O_{12}$ and $Bi_2Ti_2O_7$ phases. Above 700 °C, the films were polycrystalline $Bi_4Ti_3O_{12}$ and finally above 800 °C, the orientation was *c*-axis oriented $Bi_4Ti_3O_{12}$. Wills et al. [5] deposited titanium-rich $Bi_4Ti_3O_{12}$ thin films between 600 and 800 °C. Below 750 °C, the films were polycrystalline and above 800 °C, the multiphase films contained both $Bi_2Ti_2O_7$ and $Bi_4Ti_3O_{12}$. Similar results were obtained by Yamaguchi et al. [1].

Substrate or buffer layer effects the crystalline orientation as well as the crystallinity of the thin films. In the case of $Bi_4Ti_3O_{12}$, Yoshimura et al. [32] found that films deposited on Pt/Ti/SiO_2/Si substrate were highly *c*-axis oriented but when deposited on SiO_2/Si XRD reflections originating also from the $Bi_2Ti_2O_7$ phase were observed. Fu et al. [29] detected $Bi_2Ti_2O_7$ thin films to be randomly oriented when deposited on Si(1 0 0) substrates but 111 oriented when deposited on fused quartz. Improved crystallinity and better surface morphology were observed for $Bi_4Ti_3O_{12}$ deposition in the presence of Bi_2SiO_5 [1,33] and $Bi_2Si_2O_7$ [27] buffer layers as compared to the $Bi_4Ti_3O_{12}$ films deposited without a buffer layer.

In the atomic layer deposition (ALD) [34–36], unlike in CVD, the evaporated precursors are introduced into the reactor in alternating pulses separated by inert gas purging. The film growth proceeds by layer-by-layer manner and in an ideal case one monolayer or a distinct fraction of it is formed during each growth cycle. In practice, however, due to steric factors a full monolayer growth is not achieved. The film growth is controlled by saturative reactions of the precursor with reactive surface groups making the process self-limiting. Previously Schuisky et al. [21] have studied ALD of Bi–Ti–O from triphenylbismuth and titanium isopropoxide together with water as oxygen source. Bismuth titanates with higher Bi to Ti ratios than 0.61 were not obtained, however. Pulsed CVD, which resembles ALD, has formerly been used for the deposition of $Bi_4Ti_3O_{12}$ thin films [15]. In this method, the metal precursor vapours have been one by one mixed with the oxygen source and then separately introduced into the reaction chamber. It was found out that the films prepared by pulsed CVD method showed larger degree of *c*-axis orientation than films prepared by the conventional CVD method. Cho et al. [16] have recently introduced an ALD-related process where the metal precursors and oxidizing gas were injected and separated by inert gas purging. The dielectric constant of these films was about 320 and leakage current below 10^{-8} A/cm^2 for 140 nm thick film. However, a well-saturated hysteresis was not obtained.

In our earlier study [37], we have synthesized $Bi(CH_2SiMe_3)_3$ and introduced it as a novel ALD precursor for bismuth silicate thin films. In the present work, we have further optimized the Bi–Si–O ALD processes. In addition, we have deposited Bi–Ti–O films by ALD and studied the crystallization behaviour in Bi–Si–O as well as in the Bi–Ti–O system.

2. Experimental procedure

2.1. Film deposition and heat treatment

Thin films were deposited in a flow-type F-120 ALD reactor (ASM Microchemistry Ltd.) operated under a pressure of about 3 mbar. High-purity nitrogen (>99.999%), generated in a Nitrox UHPN 3000-1 nitrogen generator, was used as a carrier and purging gas. $Bi(CH_2SiMe_3)_3$ was used as precursor for the Bi–Si–O thin films, whereas triphenylbismuth ($BiPh_3$, Strem Chemicals, 99%) was used as the bismuth source for both Bi–Si–O and Bi–Ti–O thin films. Titanium isopropoxide ($Ti(O\text{-}i\text{-}Pr)_4$, Aldrich Chem. Co., 97%) was used as the titanium source. $Bi(CH_2SiMe_3)_3$, $BiPh_3$ and $Ti(O\text{-}i\text{-}Pr)_4$ were evaporated from open crucibles kept at 45, 115 and 40 °C, respectively. Synthesis and characterization of the $Bi(CH_2SiMe_3)_3$ precursor have recently been described in detail [37]. Ozone was generated from oxygen (>99.999%) in an ozone generator (Fischer model 502) and water was vaporized from a cylinder kept at 30 °C. Precursors, evaporation temperatures and oxidizers are summarized in Table 1.

Optimized process parameters for Bi–Si–O thin films were determined in our earlier study where the films were deposited from the $Bi(CH_2SiMe_3)_3$ precursor [37]. Based on those results, deposition temperature of 250 °C was

Table 1
Precursors, evaporation temperature of the source materials and oxidizers used

Source	Source temperature (°C)	Oxidizer
$Bi(CH_2SiMe_3)_3$	45	O_3
$BiPh_3$	115	O_3
Ti(O-i-Pr)$_4$	40	H_2O

chosen for the Bi–Si–O thin film growth from $Bi(CH_2SiMe_3)_3$, $BiPh_3$ and O_3. Deposition of Bi–Ti–O was performed at a single chosen temperature of 250 °C. The pulse length was 1 s for $BiPh_3$, Ti(O-i-Pr)$_4$ and H_2O and 1.5 s for O_3. The Bi–Si–O thin films were deposited on sapphire as well as on Si(1 0 0), which was buffered by MgO [38], ZrO_2 [39] and YSZ [40] by ALD. The Bi–Si–O samples intended for X-ray fluorescence (XRF) measurements were deposited onto Ti-foil (99.6%). The Bi–Ti–O thin films were deposited on Si(1 0 0). Rapid thermal annealing (RTA, PEO 601, ATV Technologie GmbH, Germany) was used to study the effect of heat treatment on film crystallinity and crystallite orientation. Selected Bi–Si–O thin film samples were annealed for 10 min in N_2 (>99.999%) at 600–800 °C while the Bi–Ti–O thin film samples were treated in N_2 and O_2 at 700–1000 °C. Bi–Ti–O thin films were also annealed in a tube furnace in air at 700–900 °C for 30 min.

2.2. Film characterization

Film thickness was measured from films deposited on Si(1 0 0) and buffered Si(1 0 0) substrates. Hitachi U-2000 double beam spectrometer was used to measure the reflectance spectra in the region of 190–1100 nm. Thicknesses of the deposited films on silicon were calculated from reflectance spectrum by the optical fitting method described by Ylilammi and Ranta-aho [41]. Film crystallinity and crystallite orientations were determined by powder X-ray diffraction (XRD) using Cu Kα radiation (Philips MPD 1880). Bi, Si and Ti contents were determined in Philips PW 1480 XRF spectrometer equipped with an Rh X-ray tube. In order to determine Bi and Si contents from the Bi–Si–O thin films, samples were deposited onto Ti foil (99.6%). In the case of the Bi–Ti–O thin films, Bi and Ti contents were determined from Si(1 0 0) substrates. Data analysis was performed with the Uniquant 4.34 program, which utilizes the DJ Kappa model to calculate the composition and mass thickness of an unknown thin film sample [42]. Surface morphology of selected samples was studied by Nanoscope III atomic force microscope (AFM, Digital Instruments), operating in tapping mode with a scanning frequence of 1 Hz. Roughness values were calculated as root mean square (rms) values. The concentration depth distributions and annealing behaviour of the heavier elements of the Bi–Ti–O samples were determined by an ion-beam method [43], using Rutherford backscattering spectrometry (RBS). For Bi–Si–O thin films deposited on Si(1 0 0) these have been examined earlier [37]. Also the analytical data of the metallic constituents obtained by XRF were verified by RBS. The RBS experiments were performed at the Accelerator Laboratory of the University of Helsinki, using a High Voltage Engineering 500 kV accelerator. A beam of 900 keV ^{3}He ions was employed. The RBS data analysis was carried out with the simulation codes SIMNRA and GISA [44,45].

3. Results and discussion

In our previous study [37], a constant growth rate of 0.40 Å/cycle for bismuth silicate was obtained by using $Bi(CH_2SiMe_3)_3$ and ozone as precursors at 250–350 °C. Within this temperature range according to XRF analyses, the Si to Bi atomic ratio was close to 2.0, as seen in the inset of Fig. 1. In order to increase the bismuth content in the Bi–Si–O thin films, $BiPh_3$ was used as a secondary Bi-precursor. Control of bismuth content was performed out by adding the necessary number of $BiPh_3/O_3$ cycles into the $Bi(CH_2SiMe_3)_3/O_3$ process. As seen in Fig. 1, bismuth content could be easily controlled by additional bismuth precursor.

Attempts to grow binary bismuth oxide by the $BiPh_3/O_3$ ALD process resulted in visually dark and patchy films with a steep thickness profile, nevertheless. Uniform and shiny Bi–Ti–O films were obtained, when Ti(O-i-Pr)$_4$/H_2O was used as titanium source. Similar results were obtained by Schuisky et al. [21]. Their attempts to use $BiPh_3$ together with H_2O as oxygen source to deposit bismuth oxide failed but when Ti(O-i-Pr)$_4$/H_2O was added in the process Bi–Ti–O thin films were achieved. In our experiments Bi content and Bi–Ti–O film deposition rate were constant over the substrate length of 10 cm indicating an ALD-type

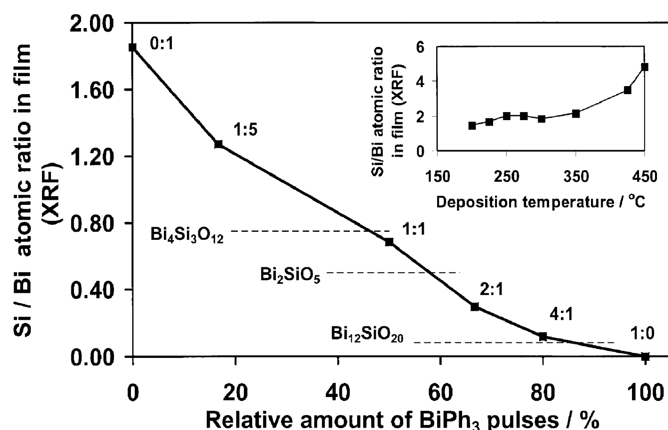

Fig. 1. Si/Bi content as a function of the pulsing ratios $Bi(CH_2SiMe_3)_3/O_3$ and $BiPh_3/O_3$. Deposition temperature was 250 °C. Inset shows the Bi/Si content in thin films as a function of the deposition temperature when the $Bi(CH_2SiMe_3)_3/O_3$ process was used. Dashed line shows Si/Bi atomic ratios in different stoichiometric bismuth silicates.

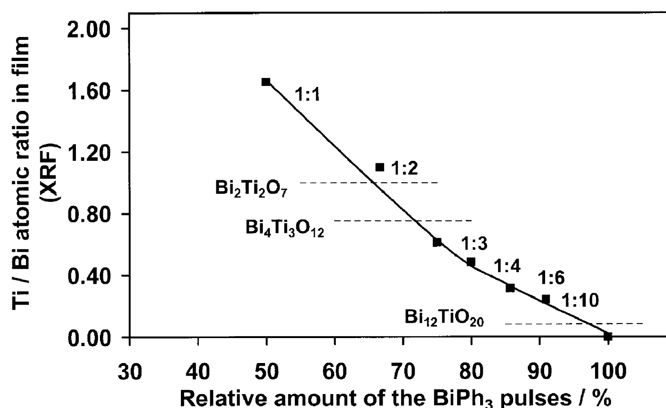

Fig. 2. Ti/Bi content as a function of the pulsing ratio of $BiPh_3/O_3$ to $Ti(O\text{-}i\text{-}Pr)_4/H_2O$. Deposition temperature was 250 °C. Dashed line shows Ti/Bi atomic ratios in different stoichiometric bismuth titanates.

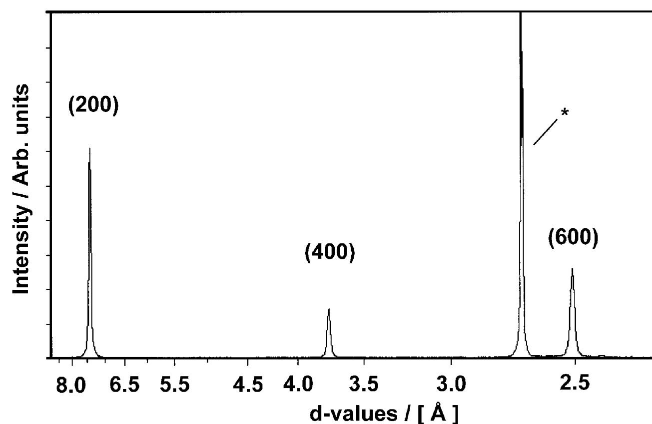

Fig. 3. XRD pattern of a 110 nm thick Bi_2SiO_5 thin film deposited on MgO-buffered Si(1 0 0) and annealed at 800 °C in N_2 atmosphere. Asterisk denotes reflection from the substrate.

growth. The XRF measurements showed that stoichiometry of the thin films could be controlled by changing the pulsing ratio of $BiPh_3/O_3$ to $Ti(O\text{-}i\text{-}Pr)_4/H_2O$ (Fig. 2).

According to XRD data, both Bi–Si–O and Bi–Ti–O thin films were amorphous after the deposition. Crystallization of the Bi–Si–O thin films was studied from samples deposited by using the $Bi(CH_2SiMe_3)_3/O_3$ process only. According to our previous annealing studies [37], crystallization begins on the Si(1 0 0) substrates at 600 °C when the films are deposited at 250 °C regardless of the atmosphere. Films were *a*-axis-oriented orthorhombic Bi_2SiO_5 but some minor peaks of the cubic $Bi_{12}SiO_{20}$ phase were also detected. At 1000 °C the presence of polycrystalline cubic $Bi_4Si_3O_{12}$ phase was observed but the films were patchy. Further annealing of the films deposited on sapphire and MgO-, ZrO_2- and YSZ-buffered Si(1 0 0) were carried out at 600–800 °C in an inert nitrogen atmosphere. Films deposited on sapphire and buffered films were all *a*-axis-oriented orthorhombic Bi_2SiO_5 without traces of the $Bi_{12}SiO_{20}$ phase. The best crystallinity was obtained when films were annealed at 800 °C. All samples were crystalline already at 600 °C except for films deposited on MgO-buffered Si(1 0 0) which started to crystallize at 700 °C.

The full-width half-maximum (FWHM) values for the strongest peaks, i.e. 200 were also studied as a function of Bi–Si–O thin film thickness. A FWHM value of 0.125° was obtained for the 200 Bi_2SiO_5 reflection when films were deposited onto 180 nm thick MgO-buffered Si(1 0 0) substrates (Fig. 3). No significant differences in the FWHM values between the 75 and 110 nm thick films were observed. As seen in Fig. 4, the AFM measurements show that the films are highly crystalline and consist of large crystals extending through the film. The other FWHM values for 200 reflection were 0.474°, 0.528° and 0.516° in sapphire, 110 nm thick ZrO_2 buffer layer on Si(1 0 0) and in 100 nm thick YSZ buffer layer Si(1 0 0), respectively. For the Bi_2SiO_5 films, peak intensities of the 200 reflection were ten times higher on MgO-buffered Si(1 0 0) than on Si substrate without the buffer layer. Thin films deposited on

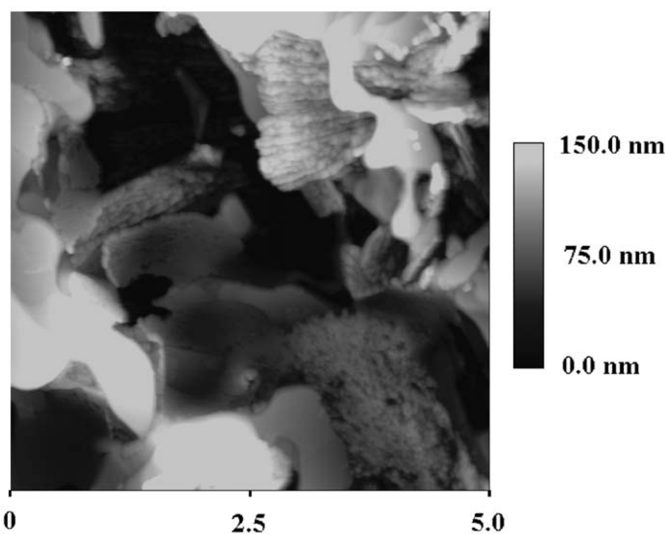

Fig. 4. AFM image of 110 nm thick Bi–Si–O film deposited on 180 nm thick MgO-buffered Si(1 0 0). Image size 5 × 5 μm². Depth scale: 150 nm from black to white.

sapphire, ZrO_2-buffered Si(1 0 0), YSZ-buffered Si(1 0 0) exhibited from 1.3 to 2.6 times higher intensities for the 200 reflection than those deposited on Si(1 0 0).

Annealing of Bi–Ti–O thin films was performed in N_2, O_2 or air. Interestingly, the film stoichiometry had a very significant effect on the crystalline phases formed when annealed in a N_2 atmosphere. Sun et al. [4] have observed that a high Bi/Ti ratio induces film growth with *c*-axis-oriented crystal structure of $Bi_4Ti_3O_{12}$. In our study, the best crystallinity of $Bi_4Ti_3O_{12}$ was obtained with an excess of bismuth (Ti/Bi atomic ratio 0.28) but films were *b*-axis oriented. It was found that a low bismuth content, i.e. Ti/Bi atomic ratio >1.0, resulted in $Bi_2Ti_2O_7$ phase formation when films were annealed at 700–800 °C. When titanium-to-bismuth atomic ratio was below 0.75, $Bi_4Ti_3O_{12}$ was crystallized but some minor peaks of $Bi_2Ti_2O_7$, $Bi_2Ti_4O_{11}$

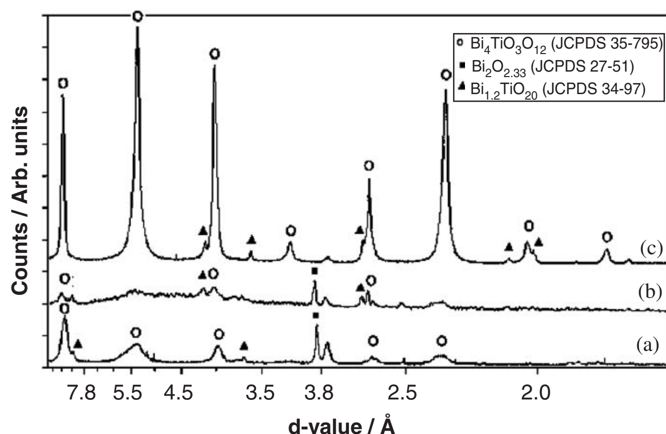

Fig. 5. XRD patterns of Bi–Ti–O thin films annealed at 800–1000 °C in N_2 atmosphere for 10 min. Bi–Ti–O films was deposited on Si(1 0 0) with pulsing ratio of 1:10 (Ti/Bi atomic ratio 0.28). Film thickness was 95 nm.

Table 2
Reflections of Bi–Ti–O phases near the *d*-value of 2.95 according to JCPDS [49]

d (Å)	(*h k l*)	Phase	JCPDS
2.980	444	$Bi_2Ti_2O_7$	32–118
2.978		$Bi_2Ti_4O_{11}$	15–325
2.970	171	$Bi_4Ti_3O_{12}$	35–795
2.935	222	$Bi_{12}TiO_{20}$	34–97

and $Bi_2O_{2.33}$ were also observed. XRD intensities from the $Bi_4Ti_3O_{12}$ phase increased as the temperature was raised. At 1000 °C only strong 0*k*0 reflections were detected together with minor peaks of the $Bi_2Ti_4O_{11}$ phase (Fig. 5). Films annealed at 1000 °C were visually shiny and flat. Adhesion of the films was tested by the tape test [46], and no peeling was observed regardless of the annealing temperature. Fig. 5 shows the effect of annealing temperature in nitrogen atmosphere. Identification of the peak at $d = 2.95$ cannot be reliably performed due to the fact that several phases have strong reflections with almost the same *d*-value (Table 2). Anyhow, the 117 reflection of $Bi_4Ti_3O_{12}$ appears to be the most probable.

Annealing in air at 700 °C for 60 min resulted in the formation of $Bi_2Ti_4O_{11}$ when bismuth content was low (atomic ratio $Ti/Bi > 0.7$). When bismuth content in the films was increased $Bi_2Ti_2O_7$ phase was detected together with a minor reflection due to $Bi_2Ti_4O_{11}$. At 900 °C, the $Bi_4Ti_3O_{12}$ phase was crystallized as highly 0*k*0 oriented with only a weak additional reflection due to the $Bi_{12}TiO_{20}$ phase. Unfortunately intensities of the XRD peaks were much weaker than after nitrogen annealing. Annealing in O_2 was performed only for films with pulsing ratio of 1:10 (Ti to Bi atomic ratio of 0.28). Films were poorly crystalline below 900 °C but at that temperature 0*k*0 oriented $Bi_4Ti_3O_{12}$ phase was observed with a few minor reflections originated from $Bi_2Ti_4O_{11}$ and $Bi_{12}TiO_{20}$.

AFM and RBS were used to examine surface morphology and distribution of bismuth in Bi–Ti–O thin films, respectively. AFM measurements showed that roughness of the films was increased with increasing bismuth content (Fig. 6). Amorphous as-deposited films with Ti/Bi atomic ratio 0.28, 0.71 and 1.28 had rms values 4.6, 2.5 and 1.8 nm, respectively. Thicknesses of these films were between 95 and 100 nm. However, there were only minor differences in the surface roughness of annealed samples caused by the atomic ratio. When annealed in nitrogen at 800 °C, rms values of 6.1 and 6.6 nm were obtained for Ti/Bi atomic ratios 0.28 and 1.28, respectively. When comparing the results obtained from as-deposited and annealed films it seems that annealing at 800 °C flattens the rough surface of films with higher bismuth content. In previous studies, Araujo et al. [47] deposited $Bi_4Ti_3O_{12}$ thin films on Si substrates by spin coating. Films were annealed at 500, 600 and 700 °C and roughness values of the films ranged from 3 to 10 nm. In the case of $Bi_4Ti_3O_{12}$, thin films were deposited by dipping pyrolysis [48] and the rms roughness values were after annealing at 750 °C, 7.0 and 14.4 nm for the $LaAlO_3$ and $SrTiO_3$ substrates, respectively.

Areal densities of 585×10^{15} and 825×10^{15} at/cm^2 were obtained from the Rutherford backscattering experiments performed on the Bi–Ti–O thin films samples with Ti/Bi atomic ratios of 0.28 and 0.71 and, respectively. For comparison, as-deposited and two annealed samples with the film content of 0.28 and 0.71 were also analysed. Atomic ratios obtained from RBS were congruent with result obtained from XRF. Figs. 7 and 8 illustrate backscattering spectra for 900 keV ^{3}He ions incident on these samples. The insets show the change in the concentration depth distributions of Bi and Ti for the as-deposited and annealed samples.

As can be observed in Figs. 7 and 8, the total Bi content is significantly reduced by the annealing procedure. The spectra and the depth distributions show a redistribution of Bi away from the interface and towards the surface. The total content of Ti remains almost unchanged for both samples, however, but a clear redistribution of Ti away from the interface to the surface is also observed for the 585×10^{15} at/cm^2 sample. These effects for Bi and Ti are more pronounced for the sample with the higher bismuth content and after annealing at 1000 °C. In the case of the 825×10^{15} at/cm^2 sample, although not definitely verified from the Ti signal, similar redistribution behavior for Ti is also probable. The total content of Ti remains almost constant in all other cases. After annealing at the higher temperature, there is some Si observable with RBS on the surface of both samples.

The Bi–Ti–O films annealed in air and in oxygen were of poor quality as observed visually, while the films annealed in nitrogen were smooth and shiny even after annealing at 1000 °C. An oxidizing atmosphere seems to deteriorate the

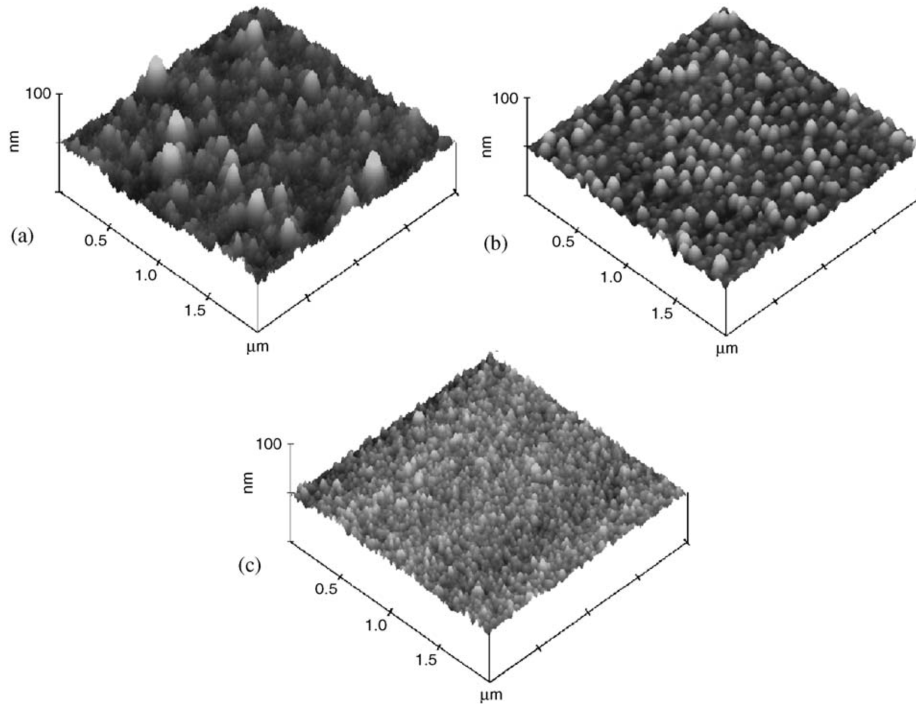

Fig. 6. AFM images of amorphous Bi–Ti–O films with a Ti/Bi atomic ratio of 0.28 (a), 0.71 (b) and 1.28 (c). The rms roughness values were 4.6 (a), 2.5 (b) and 1.8 nm (c). The Bi–Ti–O layer thickness was 95 (a) and 100 nm (b,c). Image size $2 \times 2\,\mu m^2$. Depth scale: 50 nm from black to white.

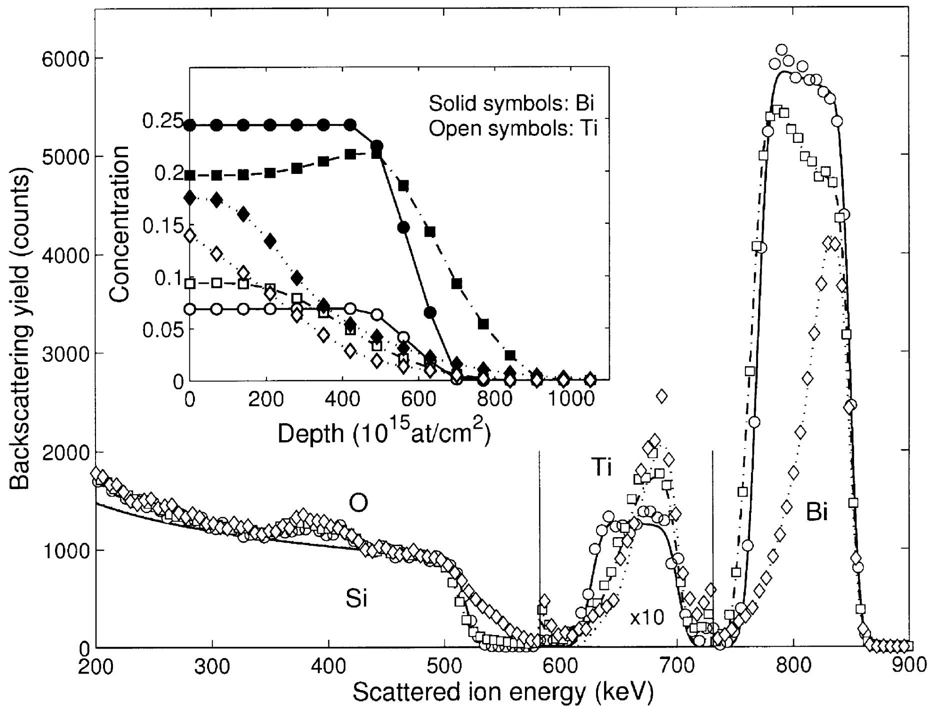

Fig. 7. Rutherford backscattering spectra for 900 keV ^{3}He ions incident on the 585×10^{15} at/cm^2 bismuth titanate sample. The inset shows the corresponding concentration depth distributions of Bi and Ti as derived from the spectra. The symbols stand for different sample preparations: Circles, as grown; squares, annealed in 800 °C; diamonds, annealed in 1000 °C. The lines connecting the experimental symbols in the spectra are the theoretical simulations; in the inset, the lines are drawn to guide the eye. The Ti signal of the spectrum has been multiplied by 10 for clarity.

Bi–Ti–O films and therefore nitrogen atmosphere is preferable. However, the annealing temperature of 1000 °C required for highly (0 k 0) oriented $Bi_4Ti_3O_{12}$ is too high for most of the applications. Also the RBS results revealed that changes in the elemental distribution after annealing at 1000 °C had occurred.

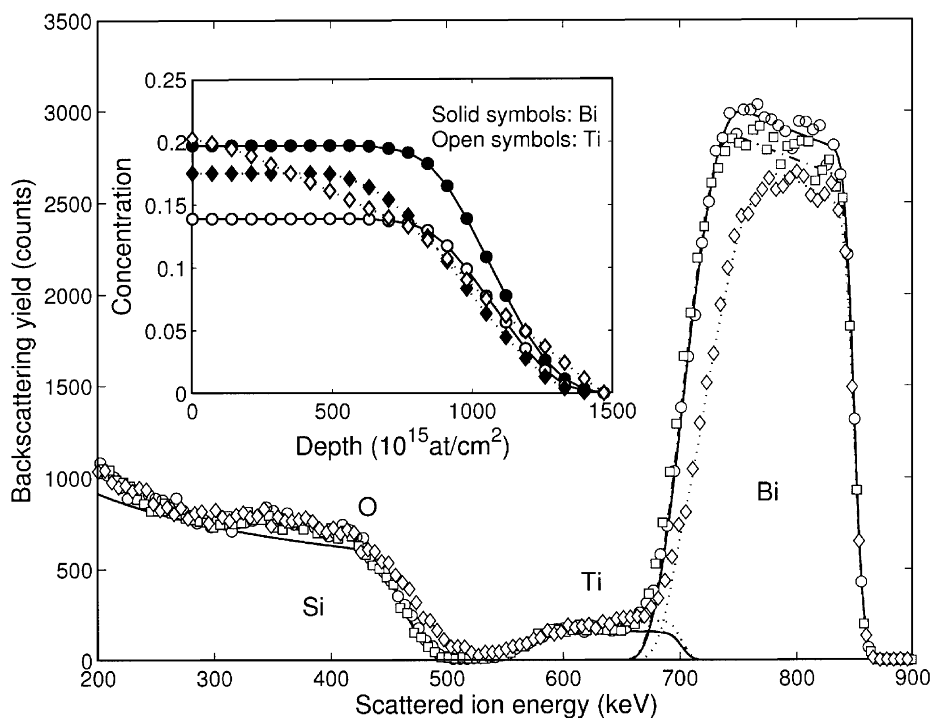

Fig. 8. Backscattering spectra for 900 keV ^3He ions incident on the 825×10^{15} at/cm^2 bismuth titanate sample as in Fig. 6. For clarity, the inset shows only the depth distributions of Bi and Ti for the as grown and the 1000 °C annealed samples.

4. Conclusions

In this study, we have investigated the control of metal ratios in the ALD growth of Bi–Si–O thin films as well as the influence of annealing on phase formation and film orientation. Bismuth content in the Bi–Si–O thin films was successfully controlled by adding $BiPh_3/O_3$ ALD cycles into the $Bi(CH_2SiMe_3)_3/O_3$ process. Sapphire as well as MgO-, ZrO_2- and YSZ-buffered Si(1 0 0) were used as substrates when the crystallization of Bi–Si–O thin films was studied. The as-deposited films were amorphous but the crystallization of Bi–Si–O thin films was initiated at 600 °C regardless of the atmosphere. The best crystallinity was obtained when films were annealed at 800 °C in a nitrogen atmosphere on MgO-buffered Si(1 0 0). The resulting films were crystalline *a*-axis-oriented orthorhombic Bi_2SiO_5. However, according to the XRF and RBS results, Bi–Si–O thin films contained more silicon than the XRD results would imply. The discrepancies between the Si/Bi ratios suggest that the thin films may also contain amorphous material.

We also studied the Bi–Ti–O thin film growth by ALD and the effect of annealing in different atmospheres on the phase formation and film orientation. $BiPh_4/O_3$ together with $Ti(O\text{-}i\text{-}Pr)_4/H_2O$ were successfully employed as precursors for the ALD deposition of bismuth titanate thin films. A good control of the film stoichiometry was achieved at the deposition temperature of 250 °C. As-deposited films were amorphous and annealing studies to crystalline them were carried out in N_2, O_2 and air for films with different stoichiometries. The best crystallinity was obtained with an excess of bismuth in N_2 atmosphere at 1000 °C. With bismuth excess, $Bi_4Ti_3O_{12}$ phase together with minor peaks of $Bi_2Ti_4O_{11}$ was observed. Nitrogen was found to be a more suitable atmosphere than oxidative environment as judged by visual appearance and adhesion of the films. Although as-deposited thin films with higher bismuth content had higher roughness values than the films with less bismuth, the roughness values balanced out after annealing at 800 °C. In spite of the fact that in Bi–Ti–O thin films the crystallinity was continuously improved up to the annealing temperature of 1000 °C this high temperature affected significantly the Bi and Ti distribution according to the RBS results. Also Si observed on the surface of thin films after annealing in such a high temperature indicates a nonequilibrium in the thin films. Because of this behaviour lower annealing temperatures or a buffer layer are recommended.

Acknowledgements

The authors are grateful to Prof. P. Hautojärvi, Department of Physics, for providing the facilities for AFM measurements and Mr. Jaakko Niinistö (M.Sc.) is thanked for help with the AFM measurements. Financial support from the Academy of Finland (projects 204742 and 205777) is gratefully acknowledged. J.H. wishes to thank the Heikki and Hilma Honkanen Foundation as well as the Finnish Foundation for Economic and Technology Sciences—KAUTE for a research stipend.

References

[1] M. Yamaguchi, T. Nagatomo, Y. Masuda, Jpn. J. Appl. Phys. 40 (2001) 5559.
[2] E.O. Klebanskii, A. Yu. Kudzin, V.M. Pasalskii, S.N. Plyaka, L. Ya. Sadovskaya, G. Kh. Sokolyanskii, Phys. Solid State 41 (1999) 913.
[3] S.W. Wang, H. Wang, X. Wu, S. Shang, M. Wang, Z. Li, W. Lu, J. Crystal Growth 224 (2001) 323.
[4] S. Sun, P. Lu, P.A. Fuierer, J. Crystal Growth 205 (1999) 177.
[5] L.A. Wills, W.A. Feil, B.W. Wessels, L.M. Tonge, T.J. Marks, J. Crystal Growth 107 (1991) 712.
[6] T. Kijima, H. Matsunaga, Jpn. J. Appl. Phys. 38 (1999) 2281.
[7] J. Kim, T. Tsurumi, T. Kamiya, M. Daimon, J. Appl. Phys. 75 (1994) 2924.
[8] K. Nomura, H. Ogawa, J. Electrochem. Soc. 138 (1991) 3696.
[9] L. Escobar-Alarcon, E. Haro-Poniatowski, M. Fernandez-Guasti, A. Perea, C.N. Afonso, T. Falcon, Appl. Phys. A 69 (1999) S949.
[10] M. Jain, A.K. Tripathi, T.C. Goel, P.K.C. Pillai, J. Mater. Sci. Lett. 18 (1999) 479.
[11] X.M. Wu, S.W. Wang, H. Wang, Z. Wang, S.X. Shang, M. Wang, Thin Solid Films 370 (2000) 30.
[12] Z. Wang, C.H. Yang, D.L. Sun, J.F. Hu, H. Wang, H.C. Chen, C.S. Fang, Mater. Sci. Eng. B 102 (2003) 335.
[13] M. Schuisky, A. Hårsta, Chem. Vap. Deposition 4 (1998) 213.
[14] H. Wang, L.W. Fu, S.X. Shang, J. Appl. Phys. 73 (1993) 7963.
[15] T. Watanabe, H. Funakubo, Jpn. J. Appl. Phys. 39 (2000) 5211.
[16] Y.J. Cho, Y.-S. Min, J.-H. Lee, B.-S. Seo, J.K. Lee, Y.S. Park, J.-H. Choi, Integrated Ferroelectrics 59 (2003) 1483.
[17] W. Jo, H.-J. Cho, T.W. Noh, B.I. Kim, D.-Y. Kim, Z.G. Khim, S.-I. Kwun, Appl. Phys. Lett. 63 (1993) 2198.
[18] M. Schuisky, A. Hårsta, S. Khartsev, A. Grishin, J. Appl. Phys. 88 (2000) 2819.
[19] J. Si, S.B. Desu, J. Appl. Phys. 73 (1993) 7910.
[20] H. Wang, L.W. Fu, S.X. Shang, X.L. Wang, M.H. Jiang, J. Phys. D 27 (1994) 393.
[21] M. Schuisky, K. Kukli, M. Ritala, A. Hårsta, M. Leskelä, Chem Vap. Deposition 6 (2000) 139.
[22] M. Yamaguchi, K. Hiraki, T. Homma, T. Nagatomo, Y. Masuda, IEEE Int. Symp. Appl. Ferroelectrics (2001) 629.
[23] Y.W. Feng, W. Hong, S.S. Xia, X.X. Hong, Y.X. Na, W. Dong, W. Min, J. Mater. Sci. Lett. 21 (2002) 1803.
[24] D.G. Papazoglou, A.G. Apostolidis, E.D. Vanidhis, Appl. Phys. B 65 (1997) 499.
[25] T. Higuchi, M. Nakamura, Y. Hachisu, M. Saitoh, T. Hattori, T. Tsukamoto, Jpn. J. Appl. Phys. 43 (2004) 6585.
[26] M.S. Tomar, R.E. Melgarejo, S.P. Singh, Microelectron. J. 36 (2005) 574.
[27] T. Nakamura, R. Muhammet, M. Shimizu, T. Shiosaki, Jpn. J. Appl. Phys. 32 (1993) 4086.
[28] S.W. Wang, H. Wang, S.X. Shang, J. Huang, Z. Wang, M. Wang, J. Crystal Growth 217 (2000) 388.
[29] L.W. Fu, H. Wang, S.X. Shang, X.L. Wang, P.M. Xu, J. Crystal Growth 139 (1994) 319.
[30] T. Kijima, M. Ushikubo, H. Matsunaga, Jpn. J. Appl. Phys. 38 (1999) 127.
[31] J. Kim, T. Tsurumi, H. Hirano, T. Kamiya, N. Mizutani, M. Daimon, Jpn. J. Appl. Phys. 32 (1993) 135.
[32] K. Yoshimura, M. Ishinabe, S. Okamura, T. Tsukamoto, Jpn. J. Appl. Phys. 34 (1995) 2425.
[33] M. Yamaguchi, T. Nagamoto, Y. Masuda, IEEE Int. Symp. Appl. Ferroelectrics (2002) 231.
[34] M. Ritala, M. Leskelä, in: H.S. Nalwa (Ed.), Handbook of Thin Film Materials, vol. 1, Academic Press, San Diego, 2002, pp. 103–159.
[35] L. Niinistö, Proc. Int. Semicond. Conf. CAS 1 (2000) 33.
[36] M. Leskelä, M. Ritala, Thin Solid Films 409 (2002) 138.
[37] J. Harjuoja, T. Hatanpää, M. Vehkamäki, S. Väyrynen, M. Putkonen, L. Niinistö, M. Ritala, M. Leskelä, E. Rauhala, Chem. Vap. Deposition 11 (2005) 362.
[38] M. Putkonen, T. Sajavaara, L. Niinistö, J. Mater. Chem. 10 (2000) 1857.
[39] M. Putkonen, L. Niinistö, J. Mater. Chem. 11 (2001) 3141.
[40] M. Putkonen, T. Sajavaara, J. Niinistö, L.-S. Johansson, L. Niinistö, J. Mater. Chem. 12 (2002) 442.
[41] M. Ylilammi, T. Ranta-aho Thin Solid Films 232 (1993) 56.
[42] UniQuant Version 2 User Manual, Omega Data Systems, Neptunus 2, NL-5505 Velhoven, The Netherlands, 1995.
[43] M. Putkonen, T. Sajavaara, L. Niinistö, J. Keinonen, Anal. Bioanal. Chem. 382 (2005) 1791.
[44] M. Mayer, Nucl. Instrum. Methods B 194 (2002) 177.
[45] J. Saarilahti, E. Rauhala, Nucl. Instrum. Methods B 64 (1992) 734.
[46] B. Chapman, J. Vac. Sci. Technol. 11 (1974) 106.
[47] E.B. Araujo, V.B. Nunes, S.I. Zanette, J.A. Eiras, Mater. Lett. 49 (2001) 108.
[48] H.-H. Ryu, K.-S. Hwang, J. Korean Phys. Soc. 40 (2002) 493.
[49] Joint Committee on Power Diffraction Standards, JCPDS, International Center for Diffraction Data, Newton Square, Pennsylvania, USA.